THE JOURNAL OF PHYSICAL CHEMISTRY B

Article

Cite This: J. Phys. Chem. B 2020, 124, 413−421

pubs.acs.org/JPCB

# Molecular Dynamics Investigation of Correlations in Ion Transport in MeTFSI/EMIM−TFSI (Me = Li, Na) Electrolytes

Piotr Kubisiak, Piotr Wróbel, and Andrzej Eilmes*

Faculty of Chemistry, Jagiellonian University, Gronostajowa 2, 30-387 Kraków, Poland

Supporting Information

**ABSTRACT:** Classical molecular dynamics simulations have been performed in polarizable and nonpolarizable force fields for series of electrolytes based on MeTFSI (Me = Li, Na) salts dissolved in EMIM−TFSI ionic liquid. Structure and dynamics of the solvation shell of $Me^+$ ions have been investigated. Contributions to the total conductivity of the electrolyte arising from motions of different ions and cross-correlations between them have been analyzed. The analysis has indicated that regardless of the type of $Me^+$ cation, motions of $Me^+$ ions and ionic liquid anions are positively correlated, contributing toward conductivity decrease and leading to negative transference numbers of metal ions. The results have confirmed experimental findings of negative transference numbers of $Li^+$ and have suggested that the effect of Me-anion correlations in certain concentration range is a general feature of $Me^+$ solutions in ionic liquids.

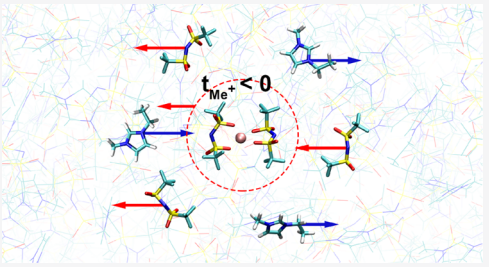


## 1. INTRODUCTION

Rechargeable metal-ion batteries have become one of the key power sources used in everyday life of a modern society, finding a vast amount of applications from mobile electronic devices to electric vehicles and energy storage systems. Since the first commercial Li-ion battery was released in the early 90s of the 20th century, continuous effort has been invested in the development of safe and reliable devices. Not only they have revolutionized our lives but they open the prospects for meeting the energy demands of a sustainable and fossil fuel-free society.[1−3] The recognition of the utmost importance of Li-ion devices has been recently expressed by the Royal Swedish Academy of Sciences awarding the 2019 Nobel Prize in Chemistry for the development of lithium-ion batteries.

An ion-conducting electrolyte is an essential component of a successful metal-ion battery, and therefore, many experimental and theoretical works were devoted to designing new electrolytes with optimized ion-transport properties.[4−7] Some concerns have been expressed regarding possible shortages in Li salt supplies in the prospect of fast growing demand; therefore, Na-ion devices have been considered as an alternative to lithium batteries.[8−11] Investigated electrolyte systems include metal salt solutions in molecular or ionic liquids (ILs) or/and polymer electrolytes.[12−15]

Transport properties of an electrolyte depend on the structure of the liquid, mutual interactions between dissolved ions, and interactions between ions and the solvent. Rational design and optimization of new systems rely, therefore, on proper understanding of ion aggregation and interactions at the molecular level.[16] The ion−ion interactions are of particular importance in ILs because they give rise to correlations between motions of ions, which may significantly affect the conductivity. In a study on Li salt solutions in EMIM-based IL, negative effective transference numbers for $Li^+$ were determined,[17] suggesting a correlation between motions of IL anions and lithium cations.

Physical insight into ion-transport processes in electrolytes may be gained from molecular dynamics (MD) simulations. Numerous MD studies on electrolytes for metal-ion batteries have been reported; here, we mention some selected recent examples for systems using ILs as solvents.[18−23] Based on MD data, diffusion coefficients and conductivities can be estimated; moreover, details on correlated ion motion can be assessed, helping to elucidate the phenomenon of negative transference numbers. Analysis of cross-correlations was used to estimate differences between transport and transference numbers in IL/molecular solvent blends[24] or to analyze $Li^+$ transport in solvate ILs.[25] In a recent work on NaFSI solutions in EMIM−FSI IL, it was demonstrated that Na−FSI correlations lead to negative effective $Na^+$ transference numbers in a range of NaFSI concentrations.[26] Several electrolytes based on lithium salts dissolved in EMIM ILs with different anions were systematically investigated using MD simulations;[27] negative $Li^+$ transference numbers were found in all systems for not too large salt concentrations.

In our work on NaTFSI solutions in EMIM−TFSI,[28] we investigated the performance of nonpolarizable and polarizable force fields (FFs) in classical MD. We showed that depending on the FF, the same effect of the conductivity decrease for higher salt fractions may originate differently from the balance of different contributions to the total conductivity. Here, we want to extend this analysis in order to check to what extent

Received: November 5, 2019
Revised: December 16, 2019
Published: December 18, 2019




DOI: 10.1021/acs.jpcb.9b10391
J. Phys. Chem. B 2020, 124, 413−421

the type of the FF affects the Me-anion correlations and the transference numbers of $Me^+$ ion. We will also compare the results for two Me ions: Li and Na, to see whether the strength of correlations depends on the metal cation.

## 2. COMPUTATIONAL DETAILS

In this work, we investigated the $Me_xEMIM_{(1-x)}TFSI$ electrolytes with Me = Li or Na. LiTFSI concentrations of 0.25 and 0.5 mol/dm$^3$ used in the experimental work[17] correspond approximately to $x$ = 0.06 and $x$ = 0.12. In addition to these systems, we studied more concentrated solutions with $x$ = 0.2 and $x$ = 0.3 and the neat EMIM−TFSI IL ($x$ = 0). In the analysis of the latter systems with Na, we reused the MD trajectories recorded in our previous work.[28] All other systems were modeled from the beginning. Initial structures were prepared using Packmol program.[29] Compositions of all systems are listed in the Supporting Information (Table S1).

MD simulations were performed in NAMD v 2.12[30] simulation package. Parameterization of the FFs was the same as used in our recent works on ILs.[28,31] Nonpolarizable FF for EMIM−TFSI liquid was based on OPLS parameterization[32] with bonded parameters taken from Lopes/Pádua field[33] and nonbonded from Köddermann's work.[34] Charges in this FF were not scaled. Nonbonded parameters for $Li^+$ and $Na^+$ were taken from ref 35. This parameterization will be denoted as NP-FF.

Based on the NP-FF, we constructed a polarizable parameterization (DP-FF) in which polarization effects are introduced via Drude oscillators.[36] Drude particles were attached to all nonhydrogen atoms of EMIM and TFSI ions. Polarizabilities of $Li^+$ and $Na^+$ ions are much smaller than the polarizabilities of other atoms in the system; therefore, for simplicity, Drude oscillators were not used for $Me^+$ ions. Atomic polarizabilities and charges were adapted from the APPLE&P polarizable FF for liquids and electrolytes.[37] Details of both parameterizations are provided in the Supporting Information.

NAMD simulations were performed in the $NpT$ ensemble at $p$ = 1 atm and $T$ = 333 K with Langevin dynamics and modified Nose−Hoover Langevin barostat.[38,39] Although the temperature of the experiment was lower,[17] we performed the simulations at 333 K (i.e., higher of the two temperatures used earlier in ref 28) in order to obtain better statistics for conductivity analysis, owing to faster dynamics at increased $T$. A time step of 1 fs was used to integrate equations of motion. Periodic boundary conditions were applied to the system, and electrostatic interactions were taken into account via the particle mesh Ewald algorithm.[40] Approx. 1100 ns of the MD trajectory were obtained for each system; with the initial 100 ns treated as the equilibration stage and the last 1000 ns used for the analysis.

## 3. RESULTS AND DISCUSSION

**3.1. Structure of Electrolytes.** Me−O radial distribution functions (RDFs) are shown in Figure 1. The first maximum of the Li−O RDF appears at 2.0 or 2.1 Å in the structures obtained in the polarizable or nonpolarizable FF, respectively. The second, lower and broader maxima are located at 4.0 and 4.5 Å, accordingly. Because of the larger radius of the $Na^+$ ion, the two peaks in the Na−O RDFs are lower but wider than in the case of Li−O distribution and shifted to larger distances: 2.5 and 4.6 Å in DP-FF simulations and 2.6 and 4.9 Å for NP-FF structures. When the concentration of $Me^+$ increases, the height of the first maximum is slightly reduced. Some small shifts (up to 0.05 Å) toward shorter distances of the second maximum of the Li−O RDF and of both maxima in Na−O RDF are observed for higher salt contents.

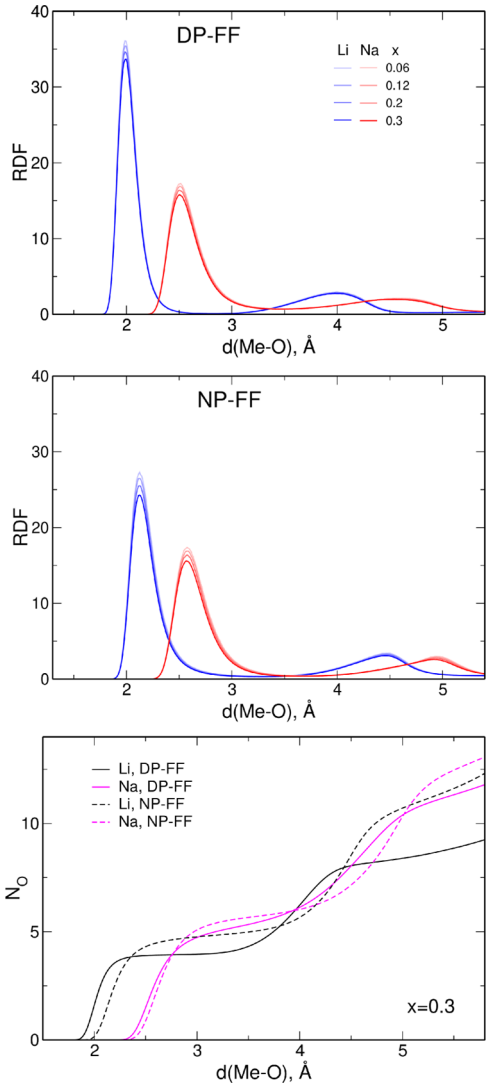


**Figure 1.** RDFs for Me−O obtained in the polarizable (top) and the nonpolarizable FF (middle); integrated Me−O RDFs for $x$ = 0.3 (bottom).

Integrated RDFs [running coordination numbers (CNs) of $Me^+$ ions] for distances smaller than 6 Å practically do not depend on salt concentration; the values obtained for electrolytes with $x$ = 0.3 are presented in the bottom panel of Figure 1. The number of oxygen atoms in the first coordination shell of Na ion is larger than for the Li ion, consistently with a smaller radius of the latter cation. At the distance of 3 Å from the central Li ion, there are on average 3.96 oxygen atoms in DP-FF and 4.76 atoms in NP-FF simulations. Corresponding values for Na−O RDF at the distance of 3.5 Å are 5.34 and 5.66 atoms, respectively. CNs are, therefore, larger in nonpolarizable simulations, and the effect of accounting on polarization effects in simulations is similar to the decrease of the ion radius: a shift of the maximum in the Me−O RDF to smaller distances with a decrease of the number of coordinating oxygens.



DOI: 10.1021/acs.jpcb.9b10391
J. Phys. Chem. B 2020, 124, 413−421

From the data for both cations shown in Figure 1, we can conclude that in the polarizable FF, both maxima in the RDFs shift to lower distances. For the first maximum, we attribute the effect to stronger $Me^+$−anion interactions. As a result, the first solvation shell is tighter. As we will see from the analysis of CNs, polarizable FF favors multidentate coordination, therefore the first shell is more compact. This in turn, for geometrical reasons, allows the anions from the 2nd shell to closer approach the $Me^+$ cation. Accordingly, as seen in Figure 1, in the DP-FF, both 1st and 2nd shells contain less oxygen atoms with respect to NP-FF results.

Some more information on the coordination of Me cations can be obtained from the histograms of the number oxygen atoms $N_O$ or the number of TFSI anions $N_{an}$ coordinated to metal ion (Figures 2 and 3); in the Supporting Information, we

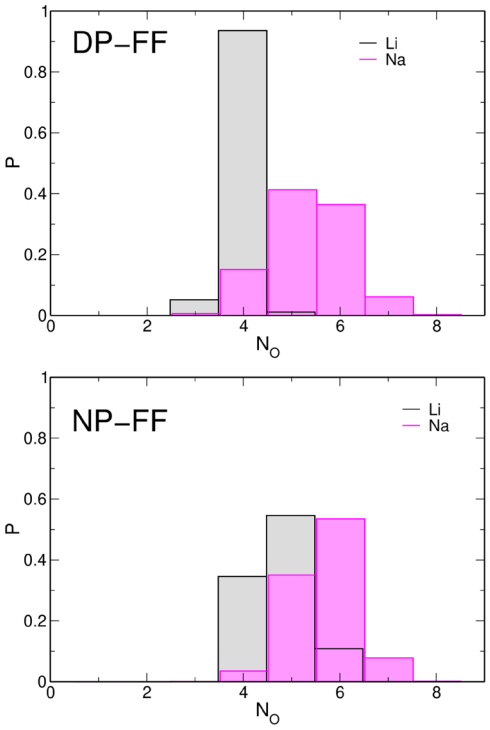


**Figure 2.** Histograms of the number of oxygen atoms coordinating the Me ions in the $x$ = 0.3 electrolytes.

present additional information on the abundance of different combinations of $N_O$ and $N_{an}$ values (Fig. S1). For this purpose, we define that the oxygen atom from the anion is coordinated to the $Me^+$ ion if the Me−O distance is smaller than 3 or 3.5 Å for Me = Li or Me = Na, respectively. The TFSI anion is counted as coordinated to the $Me^+$ if any of its O atoms fulfill the above criterion. In the structures obtained from the DP-FF, more than 90% of Li ions is coordinated to four oxygen atoms. Most of Na ions have five (40% of $Na^+$) or six (35%) oxygens in their coordination shell, but the abundance of CNs 4 or 7 is also non-negligible. The most probable number of anions coordinating the metal cation is 2 or 3 for Li or Na cations, respectively. Analysis of these values leads to the conclusion that in the DP simulations, coordination of TFSI anions to $Li^+$ is bidentate. The bidentate coordination also prevails in the solvation shell of $Na^+$: most probable is bidentate coordination to two anions with the monodentate binding of the third TFSI (CN = 5) or bidentate binding by three anions (CN = 6). The

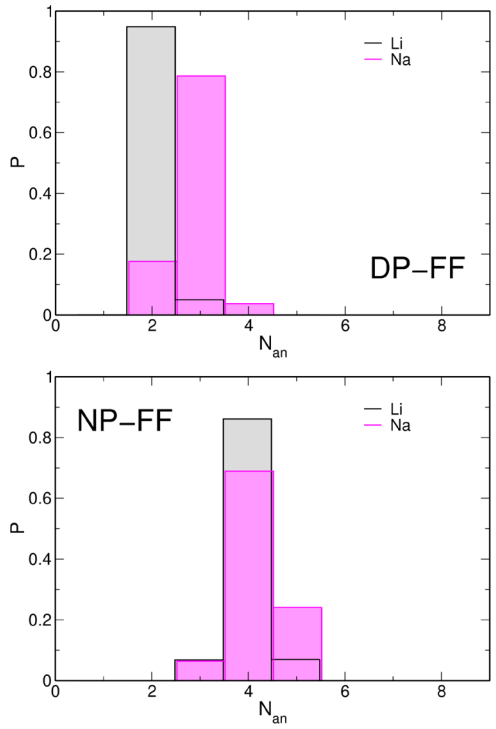


**Figure 3.** Histograms of the number of TFSI anions coordinating the Me ions in the $x$ = 0.3 electrolytes.

CNs increase in nonpolarizable simulations in the NP-FF. Most probable numbers of coordinating O atoms are 5 or 4 for Li and 6 or 5 for Na ions. Both types of $Me^+$ ions are in most cases coordinated to four TFSI anions (90% of $Li^+$ and 70% of $Na^+$). From these data, we can conclude that NP-FF increases the preference of monodentate coordination. In the most probable configurations, either all of four TFSI anions interact with $Li^+$ in a monodentate manner or one anion is involved in bidentate and three other in monodentate coordination. In the case of $Na^+$ ions, interactions with one or two TFSI anions are bidentate, and three or two other anions are bound as monodentate.

To get some insight into the dynamics of anion exchange in the solvation shells, we calculated the residence time autocorrelation function

$$C_{Me-O}(t) = \frac{\langle H_{ij}(t)H_{ij}(0)\rangle}{\langle H_{ij}(0)H_{ij}(0)\rangle} \quad (1)$$

where $H_{ij}(t)$ = 1, if the distance between $i$th $Me^+$ ion and the $j$th O atom is smaller than the threshold value or $H_{ij}(t)$ = 0 otherwise. Threshold values were 3 Å for $Li^+$ and 3.5 Å for $Na^+$.

Plots of $C_{Me-O}$ for Li and Na ions in DP and NP simulations are shown in Figure 4. The decay of the correlation function for $Li^+$ is slower than for Na ions, which may be rationalized by stronger interactions between TFSI anions and smaller Li cation. The increase of salt concentration slows further the exchange of O atoms in the coordination shell of $Li^+$, whereas this effect is smaller for $Na^+$. In particular, in the polarizable field, there is practically no concentration dependence of the O dynamics around the $Na^+$ cation. More quantitatively, these data may be characterized by oxygen atom residence times $\tau_O$ obtained by fitting the stretched exponential function $\exp[-(t/\tau_O)^\alpha]$ to $C_{Me-O}(t)$. Likewise, the anion residence times $\tau_{an}$ were


DOI: 10.1021/acs.jpcb.9b10391
J. Phys. Chem. B 2020, 124, 413−421

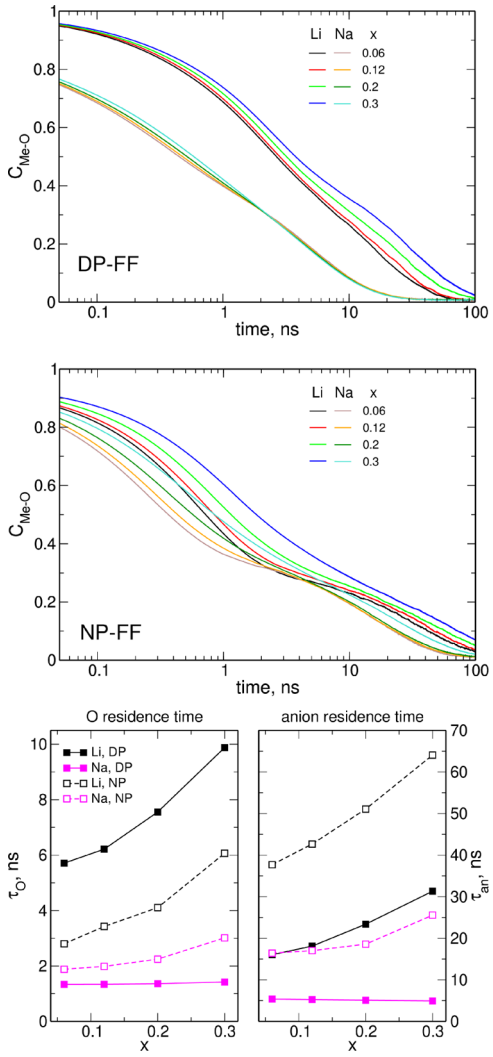


**Figure 4.** Residence time autocorrelation functions for Me−O obtained in the polarizable (top) and the nonpolarizable FF (middle); residence times $\tau$ for O atoms and TFSI anions (bottom).

calculated from the $C_{Me-an}(t)$, where $H_{ij}(t) = 1$, if the $j$th TFSI anion is coordinated to $i$th $Me^+$, that is, if any of the O atoms from the anion is within the threshold distance to $Me^+$. Plots of $C_{Me-an}(t)$ and examples of fitting results are included in the Supporting Information (Figures S2−S4), and the residence times $\tau_O$ and $\tau_{an}$ are shown in Figure 4. Residence times for anions are 3−10 times larger than $\tau_O$ because the exchange of an anion implies breaking interactions between all its O atoms and the metal cation. In all cases, residence times for interactions with $Li^+$ are 4−8 times larger than those for $Na^+$; the latter are also much less dependent on salt concentration. We can conclude, therefore, that the anion exchange in the solvation shell of the metal cation is significantly faster in the case of $Na^+$.

**3.2. Ion Transport.** Diffusion coefficients were estimated from the MD trajectories: the diffusion coefficient $D_i$ of ion $i$ was calculated from the slope of the time dependence of its mean square displacement (MSD)

$$D_i = \lim_{t\to\infty} \frac{1}{6t}\langle|\boldsymbol{R}_i(t) - \boldsymbol{R}_i(0)|^2\rangle \quad (2)$$

Conductivity of the system was calculated from the Einstein relation as

$$\sigma = \lim_{t\to\infty} \frac{e^2}{6tVk_BT}\sum_{i,j} z_i z_j \langle[\boldsymbol{R}_i(t) - \boldsymbol{R}_i(0)][\boldsymbol{R}_j(t) - \boldsymbol{R}_j(0)]\rangle \quad (3)$$

In the above formulas, $t$ stands for time, $V$ is the volume of the simulation box, $k_B$ is the Boltzmann's constant, $T$ is the temperature, $e$ is the elementary charge, $z_i$ and $z_j$ are the charges of ions $i$ and $j$, $\boldsymbol{R}_i(t)$ is the position of $i$-th ion at time $t$, and the brackets $\langle\rangle$ denote the ensemble average.

The conductivity is proportional to the collective ion diffusion coefficient

$$D_{coll} = \lim_{t\to\infty} \frac{1}{6tN}\sum_{i,j} z_i z_j \langle[\boldsymbol{R}_i(t) - \boldsymbol{R}_i(0)][\boldsymbol{R}_j(t) - \boldsymbol{R}_j(0)]\rangle \quad (4)$$

$N$ is the total number of ions in the system. $D_{coll}$ would reduce to the average of anion and cation diffusion coefficients $D_{avg} = (D_- + D_+)/2$ if there is no correlation between movements of different ions, that is, when the off-diagonal terms in eq 4 are negligibly small.

The 1 $\mu$s long MD trajectories were split into parts of 100 ns each, and the MSDs were averaged over all 10 parts. An example is shown in the Supporting Information (Figure S5); the averaged MSD is much more linear than MSD of individual parts. It is also readily seen that slopes of different parts of the trajectory may differ quite significantly. We used the standard deviation obtained for the set of 10 individual parts as the uncertainty estimate of the average value.

Diffusion coefficients estimated from the MD simulations in the DP and NP FFs are shown in Figure 5. Values obtained in polarizable simulations depend only a little on the electrolyte concentration. On the other hand, coefficients calculated from the NP-FF data readily decrease with increasing salt content. For the neat EMIM−TFSI, the NP-FF values are about 80% of the coefficients obtained in DP-FF; this difference increases with increasing $x$. In all cases, the highest mobility is predicted

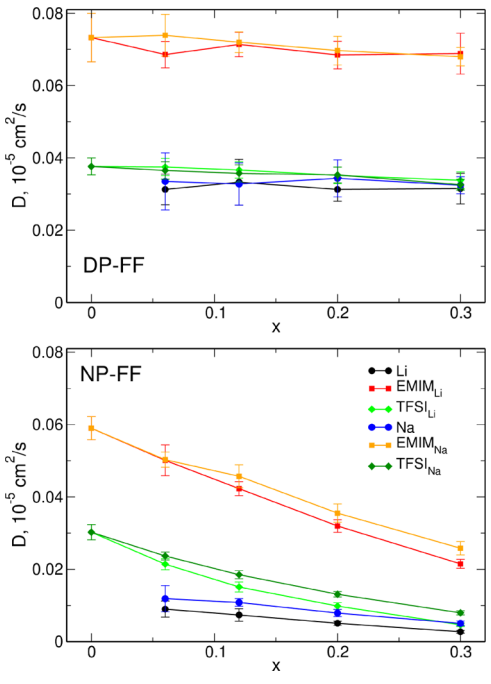


**Figure 5.** Calculated diffusion coefficients of ions.



DOI: 10.1021/acs.jpcb.9b10391
J. Phys. Chem. B 2020, 124, 413−421

for the EMIM cation; diffusion coefficients for the TFSI anion and the metal cations are about two times smaller. In nonpolarizable simulations, diffusion coefficients for all species in the electrolytes based on Li salt seem to be systematically lower than in systems with NaTFSI; conversely, there is no evident difference in DP-FF simulations. $D_{Me}$ obtained in the DP-FF is very close to $D_{TFSI}$, suggesting that the motions of both types of ions may be correlated. In NP-FF simulations, the diffusivity of Me cations at lower salt contents is substantially smaller than $D_{TFSI}$; mobilities of $Me^+$ and TFSI are getting closer in concentrated electrolytes.

Estimated conductivities of all studied systems are displayed in Figure 6. We marked the experimental values (from ref 41 for Na and from ref 42 for Li) available for the temperature of our simulations. Because of large uncertainties, it is not easy to compare the data and to detect the trends. Nevertheless, it may be noted that the nonpolarizable simulations yield conductivities lower than the calculations in the DP-FF, consistently with the difference in diffusion coefficients. For both types of Me ions in both parameterizations, the conductivity of the system generally decreases with increasing content of MeTFSI salt. We will see from the following analysis of the collective motions of ions that this decrease, although looking similar in DP and NP FFs, has different origin depending on the FF parameterization. The measured values for small $x$ are larger than calculated (thus DP-FF is closer to the experiment), but for $x = 0.2$ and $x = 0.3$, the DP-FF results for NaTFSI electrolytes agree well with the experiment. We shall also mention that the EMIM−TFSI conductivity obtained in ref 27 is close to our DP-FF value, but for increasing $x$, it decreases faster than in our results.

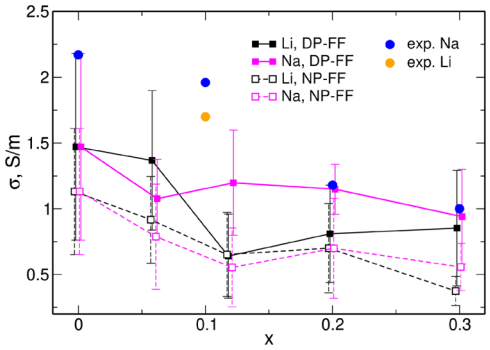


**Figure 6.** Conductivities of the $Me_xEMIM_{(1-x)}TFSI$ electrolytes calculated in two FFs.

The sum used to calculate the conductivity in eq 3 or the collective MSD in eq 4 may be decomposed into contributions with $i = j$ (diagonal components)—related to diffusion of individual ions and off-diagonal components with $i \neq j$ arising from correlations between motions of different ions; the off-diagonal terms include cross-correlations between ions of the same type and cross-correlations between ions of different types. In an extreme case, when the movements of ions are completely uncorrelated, the sum of off-diagonal components will be 0, and the collective diffusion coefficient would reduce to the average of diffusion coefficients of anions and cations, for example, $(D_+ + D_-)/2$ for the binary system $C^+A^-$. It is therefore generally accepted that the difference between the collective and the average diffusion coefficients is the measure of the degree of correlated motion in the system. Indeed, a large difference between $D_{coll}$ and $D_{avg}$ indicates strong correlations (large absolute value of off-diagonal terms in eq 3). However, the opposite is not always true because of the possible cancellation of the off-diagonal components in the system with significant correlations.

In Figure 7, we show the contributions to the total conductivity of investigated systems arising from different parts of the sum in eq 3. For this purpose, the conductivity has been partitioned into diagonal terms $\sigma_{Me}$, $\sigma_{EMIM}$, and $\sigma_a$ related to self-diffusion of $Me^+$, EMIM, and TFSI ions, respectively, the and off-diagonal terms arising form correlations between different ions: anion−anion ($\sigma_{a-a}$), cation−cation ($\sigma_{c-c}$), and cation−anion ($\sigma_{c-a}$)

$$\sigma = \sigma_{Me} + \sigma_{EMIM} + \sigma_a + \sigma_{a-a} + \sigma_{c-c} + \sigma_{c-a} \quad (5)$$

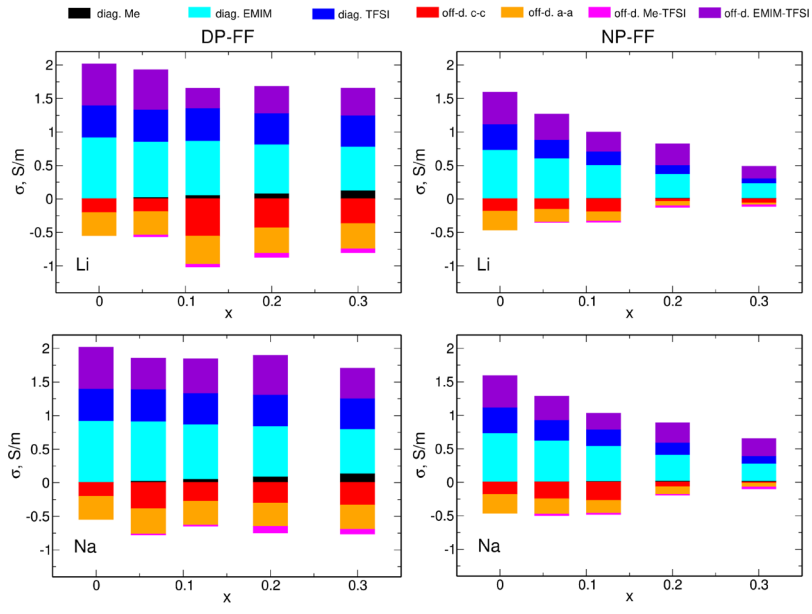


**Figure 7.** Contributions to the total conductivity of the $Me_xEMIM_{(1-x)}TFSI$ electrolytes obtained in two FFs.



DOI: 10.1021/acs.jpcb.9b10391
J. Phys. Chem. B 2020, 124, 413−421

the $\sigma_{c-a}$ contribution was further divided into parts related to Me−TFSI and EMIM−TFSI correlations

$$\sigma_{c-a} = \sigma_{Me-a} + \sigma_{EMIM-a} \quad (6)$$

Likewise, the off-diagonal $\sigma_{c-c}$ contribution may be decomposed into $\sigma_{Me-Me}$, $\sigma_{Me-EMIM}$, and $\sigma_{EMIM-EMIM}$ terms

$$\sigma_{c-a} = \sigma_{Me-Me} + \sigma_{Me-EMIM} + \sigma_{EMIM-EMIM} \quad (7)$$

describing the correlations between Me−Me, Me−EMIM, and EMIM−EMIM ions, respectively. We should also note that in the literature,[25,43] the diagonal terms $\sigma_{Me}$, $\sigma_{EMIM}$, and $\sigma_a$ are often referred to as "self" contributions, whereas the $\sigma_{Me-Me}$, $\sigma_{EMIM-EMIM}$, and $\sigma_{a-a}$ are named "distinct" contributions. For convenience, we include in the Supporting Information, a scheme of different contributions shown in Figure 7.

Let us recall some general features of different contributions to the conductivity. The diagonal contributions, being a sum of squares, are always non-negative; therefore, they positively contribute to the total conductivity. Anticorrelated motions of ions of the same charge result in negative values of the off-diagonal anion−anion and cation−cation terms both in ILs and in salt solutions in molecular solvents. These two types of electrolytes differ in the sign of the off-diagonal cation−anion component. In molecular solvents, motions of cations and anions are positively correlated, and the $\sigma_{c-a}$ is negative. Therefore in these electrolytes, the effect of all correlations is destructive for the conductivity. However, in ILs, the momentum conservation requires that cation−anion motions are anticorrelated, and the $\sigma_{c-a}$ contribution is positive.[43] This can be readily seen in Figure 7 for $x = 0$ in both FFs. It can also be noted that the sum $\sigma_{a-a} + \sigma_{c-c}$ approximately equals $\sigma_{c-a}$; thus the off-diagonal contributions cancel almost completely, even though in total, they are about 80% of the size of the sum of diagonal contributions. From this example, it is evident that in ILs, the $D_{coll}$ may be close to $D_{av}$, even if the correlations between ion motions are large (large absolute values of off-diagonal contributions to the sum eq 3).

In the polarizable FF, the sum of the diagonal contributions to the conductivity is approximately constant as a result of small dependence of the diffusion coefficients on the Me salt concentration. With increasing $x$, the $\sigma_{Me}$ contribution increases at the expense of $\sigma_{EMIM}$, reflecting the changes in the fraction of different cations in the electrolyte. Diffusion coefficient for EMIM is larger than for $Me^+$, therefore, the sum of $\sigma_{Me} + \sigma_{EMIM}$ decreases slightly for larger $x$, where the $Me^+$ ions replace EMIM cations. Likewise, because of a small number of $Me^+$ ions compared to TFSI anions, the $\sigma_{Me}$ contribution is much smaller than $\sigma_a$, even though the self-diffusion coefficients of both ions are similar. The negative off-diagonal cation−cation and anion−anion contributions increase in the solutions with larger salt concentration. The cation−anion contributions arising from different types of cations differ in sign: the larger EMIM−TFSI term is positive, whereas much smaller Me−TFSI component is negative. Nevertheless, the sum of off-diagonal cation−anion terms is always positive; therefore, cation−anion correlations contribute toward increasing the total conductivity, as generally observed in ILs. For $x = 0$, the positive and the negative off-diagonal contributions cancel, and therefore the correlations do not significantly affect the conductivity of the neat EMIM−TFSI IL. When $x$ increases, the size of negative off-diagonal terms related to correlations between motions of ions of the same charge increases; simultaneously, the positive term arising from EMIM−TFSI correlations becomes smaller. As a result, the destructive off-diagonal contributions prevail, and the conductivity is suppressed in electrolytes with larger Me content.

Diffusion coefficients obtained from nonpolarizable simulations decrease with salt concentration; accordingly, all $\sigma_i$ contributions to the conductivity decrease for high $x$. The net effect of off-diagonal components for $x \geq 0.2$ is constructive, yet the conductivity of the electrolyte is reduced because of smaller diagonal contributions. We see, therefore, that both parameterizations predict a decrease of $\sigma$ for larger $x$, but the origin of the effect is different: increasing destructive net effect of correlations in the polarizable FF and decreasing mobility of ions in the nonpolarizable FF.

For completeness, we present in the Supporting Information the breakdown of the off-diagonal cation−cation $\sigma_{c-c}$ component (red areas in Figure 7) into $\sigma_{Me-Me}$, $\sigma_{Me-EMIM}$, and $\sigma_{EMIM-EMIM}$ (Figure S6). Regardless of the FF and the Me ion, the EMIM−EMIM contribution decreases, and the Me−EMIM component generally increases for larger $x$, where the fraction of EMIM ions is smaller. The $\sigma_{Me-Me}$ terms (the "distinct" contributions) are negative; therefore they act oppositely to self contributions, and reduce the total conductivity.

Finally, we will analyze the Me−TFSI contribution $\sigma_{Me-a}$ in more detail. In all systems and in both FFs, it is always negative. This does not contradict the general observation that the cation−anion correlations in ILs enhance the conductivity because the momentum conservation requirement applies to the ions of the IL solvent and not necessarily to the relatively small fraction of dissolved Me ions (the momentum balance is assured owing to motions of the solvent ions—with this respect, the situation of the dissolved Me cations resembles the salt solutions in classical molecular liquids). The negative value of the $\sigma_{Me-a}$ contribution arising from collective motions of ions of opposite charges implies that the displacements of Me and TFSI ions are positively correlated.

The $\sigma_{Me-a}$ values depend on the ratio of different ions and in order to compare the degree of correlated motion of Me and TFSI ions, the data should be normalized. In analogy to the diffusion coefficients of a given type of ions being averages over all individual ions, we calculated the average $d_{coll}^{M-A}$ contribution to the collective diffusion coefficient per one Me−anion interaction/pair. The results are shown in the upper panel of Figure 8. As the uncertainties are large, only general trends can be observed. It seems that for $x > 0.1$, there is no significant difference between Li and Na ions (for $x = 0.06$, the statistics is worse because of the smaller number of Me ions). It may be noted that the values obtained in the nonpolarizable FF are smaller, and this effect appears to be the consequence of slower ion dynamics in this FF, reducing all diffusion coefficients. Apparently, the effect of correlated movements of Me ions and IL anions is general for different Me ions and electrolyte compositions and may be observed both in polarizable or nonpolarizable simulations.

We calculated also the transference numbers from the $\sigma_i$ contributions to the total conductivity $\sigma$, for example, the $Me^+$ transference number

$$t_{Me} = (\sigma_{Me} + \sigma_{Me-Me} + \sigma_{Me-EMIM}/2 + \sigma_{Me-a}/2)/\sigma \quad (8)$$

and using analogous formulas for $t_E$ and $t_{TFSI}$. The negative "distinct" term $\sigma_{Me\text{-}Me}$ contributes toward decrease of $t_{Me}$.



DOI: 10.1021/acs.jpcb.9b10391
J. Phys. Chem. B 2020, 124, 413−421

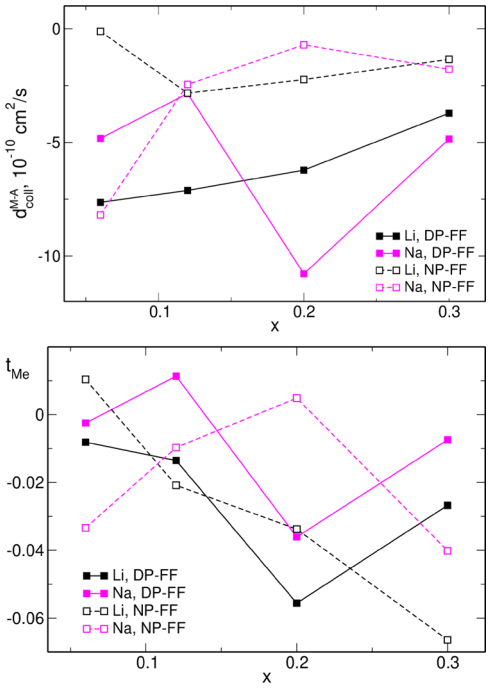


**Figure 8.** Average contributions to the collective diffusion coefficient per one Me-anion pair (top); transference numbers for $Me^+$ ions (bottom).

The $t_E$ and $t_{TFSI}$ obtained for the neat EMIM−TFSI in both fields are 0.7 and 0.3, respectively. In electrolytes with MeTFSI, $t_E$ is between 0.68 and 0.75, and the values of $t_{TFSI}$ are in the range 0.3−0.32. Values of $t_{Me}$ are shown in the lower panel of Figure 8. Because off-diagonal contributions $\sigma_i$ have relatively large uncertainties, and small values of $t_{Me}$ result from the balance of several larger terms, the data in Figure 8 suffer from large error bars and hardly any trend can be noticed. This is not surprising because the results of ref 27 show that in the whole set of investigated ILs, the effect of negative transference numbers is the smallest for LiTFSI/EMIM−TFSI electrolytes. Nevertheless, except for few points for which $d_{coll}^{M-A}$was exceptionally small (e.g., $x$ = 0.06 for Li in NP-FF), most values are negative between −0.01 and −0.06. Unlike $d_{coll}^{M-A}$, there is no apparent difference between DP and NP FFs because smaller ion mobilities in NP-FF reduce $\sigma_i$ and their sum $\sigma$ as well, therefore the ratio in eq 8 is not much affected. The effect of negative transference numbers of $Me^+$ can be therefore observed in both FFs and both for $Li^+$ and $Na^+$ ions.

Following the concept of $Me^+$ effective charges, we used the approach presented in ref 27 to estimate the cation effective charges $q_{eff}$ by comparing the $Me^+$ conductivities obtained from the uncorrelated approach to the transference numbers calculated from the full analysis of correlations in the electrolyte. The $q_{eff}$ values are expected to be greater than 1-$N$, where $N$ is the number of anions in the $Me^+$−anions cluster; faster exchange of anions will increase $q_{eff}$. The results are presented in the Figure S7 in the Supporting Information. The errors are supposed to be large because of large uncertainties of $t_{Me}$ values; nevertheless, some trends can be noticed. Typically, values for $Na^+$ are higher (less negative) than for $Li^+$ cations. The effective charges are more negative in the nonpolarizable FF compared to the DP-FF data. Both observations are consistent with the larger number of coordinating anions and slower dynamics of the solvation shell predicted in the NP-FF and with shorter anion residence times obtained for $Na^+$ ions.

**3.3. Discussion.** In ref 28, we concluded that the performance of the DP and NP FFs with respect to experimental data for NaTFSI/IL systems depends on the investigated property. Trends observed in the results obtained for LiTFSI are similar. In particular, the diffusion coefficients reported in the Supporting Information of ref 17 for $Li^+$, EMIM and TFSI ions in Li/EMIM−TFSI decrease with increasing salt content. In our MD results, such a decrease is observed in the NP-FF, whereas in DP-FF, it is very small. The nonpolarizable FF seems to reproduce the trend better; however, we shall note that the simulations were performed for temperature higher than the experiment, and the results of ref 28 for NaTFSI show that at lower temperatures, both fields exhibit the dependence of $D_i$ on $x$.

According to experimental data of ref 17, the ratio $D_{TFSI}/D_{Li}$ for $x$ = 0.06 or $x$ = 0.12 is about 1.9−1.8. In the DP-FF results, it is between 1.2 and 1.1, and the NP-FF estimates give $D_{TFSI}/D_{Li}$ = 2.4 for $x$ = 0.06 and 2.1 for $x$ = 0.12. The experimental value is therefore between predictions of the two FFs but closer to the NP-FF estimate.

Although the NP-FF may better describe the trends in changes of $D_i$, the polarizable DP-FF performs better in quantitative estimates of diffusion coefficients and conductivities. Both FFs predict too small ion mobilities and conductivities of electrolytes, but values from the polarizable simulations are higher, thus closer to measured data. In principle, the diffusion coefficients obtained for small simulation boxes are too small and should be corrected for system-size effects related to hydrodynamic interactions. For a cubic box of length $L$ such correction reads $2.837k_BT/6\pi\eta L$, where $\eta$ is the viscosity of the electrolyte.[44] For our systems, this correction amounts between 10 and 30% (for the systems with the lowest viscosities) of the computed $D_i$ values, improving the agreement with the experiment. However, a study on the size effects in MD simulations[45] showed that for ILs, the linear dependence of $D$ on $L^{-1}$ holds for system sizes larger than used in our work and therefore our estimates of the system-size corrections constitute an upper limit of the effect, and the actual corrections are smaller.

The DP-FF predictions on preferred coordination of Li cations better agree with the findings of ref 17. The most probable bidentate binding of two anions results in formation of $[Li(TFSI)_2]^-$ complexes, whereas the most probable coordination of 4 TFSI in the NP-FF predicts the appearance of $[Li(TFSI)_4]^{3-}$ aggregates. The former result is in agreement with the conclusion[17] that the "effective" charge of Li in EMIM−TFSI is −1.

Structure of the Me solvation shell differs between Li and Na, and the stability of Me−TFSI aggregates is different: Na cations exchange the anions much faster than smaller $Li^+$, as evidenced by the residence times. Differences are also observed for a given type of Me cation between different FFs. However, regardless of the metal cation and the FF used in MD simulations, the $\sigma_{Me-a}$ contribution to the conductivity in all systems is negative, indicating that the diffusion of $Me^+$ is positively correlated with motions of TFSI ions and the Me ions are transported in negatively charged aggregates. No significant difference in $\sigma_{Me-a}$ between Li and Na, despite lower residence times obtained for the latter cation suggests that the rate of exchange of TFSI ions in the solvation shell does not affect the correlations. As noted in Section 3.2, the



DOI: 10.1021/acs.jpcb.9b10391
J. Phys. Chem. B 2020, 124, 413−421

NP-FF seems to reduce the $d_{coll}^{M-A}$ by decreasing ion mobilities, but the Me−TFSI correlations persist.

Therefore, the correlated motions of $Me^+$ and IL anions in complexes with negative net charge seem to be a robust feature of salt solutions in ILs, consistent with experimental observations of "wrong" direction of $Me^+$ diffusion and negative cation transference numbers in IL-based electrolytes. We should note that this effect must be limited to a range of sufficiently low salt concentrations. Above certain salt fraction, instead of a salt solution in an IL, the system resembles molten salt with dissolved IL, and based on momentum conservation argument (ref 43), Me and anion motions will become anticorrelated, contributing positively to the conductivity. In this work, we studied only low salt concentrations, but the effect of high salt contents was presented in ref 26 for Na−FSI: around $x = 0.5$, the sign of the Na−FSI contribution changes. Likewise, the $Li^+$ transference numbers calculated in ref 27 for electrolytes with different anions change from the negative to positive at salt concentrations between $x = 0.6$ and $x = 0.7$.

The calculated $t_E$ and $t_{TFSI}$ values in EMIM−TFSI and MeTFSI solutions are about 0.7 and 0.3. The difference to the experimental data of ref 17, is up to 0.1, that is, less than cumulated uncertainties of the experiment and the simulations. The range of $Me^+$ transference numbers obtained in this work agrees well with values −0.02 to −0.04 measured for $Li^+$. The MD simulations confirm, therefore, the experimental observation of negative effective transference numbers of metal cations dissolved in ILs. Our DP-FF estimates of $t_{Li}$ in LiTFSI/EMIM−TFSI, yielding in most cases the values between −0.01 and −0.025, generally agree also with findings of ref 27. Likewise, the effective charges of $Li^+$ cation obtained from the DP-FF estimates are between −1 and −0.5, therefore agree with LiTFSI results of ref 27 presented for $x$ between 0.1 and 0.3 (on the other hand, we did not observe more negative $q_{eff}(Li)$ values for $x < 0.1$).

## 4. CONCLUSIONS

We performed classical MD simulations of LiTFSI or NaTFSI salt solutions in EMIM−TFSI IL using polarizable and nonpolarizable FFs. Apart from the difference in CNs of $Me^+$ ions related to the larger radius of $Na^+$ cation, we observed that in the nonpolarizable FF, average CNs increase. In the polarizable FF, there is a preference toward bidentate coordination of the cation, whereas NP-FF increases the fraction of monodentate interactions between the metal cation and TFSI anions. The exchange of anions in the solvation shell of $Na^+$ is faster than in the case of $Li^+$ ion; the dynamics of the solvation shell predicted by the NP-FF is slower than in polarizable simulations.

Although, in general, cation−anion motions in ILs are anticorrelated and increase the conductivity, analysis of the contributions to the total conductivity of studied electrolytes arising from cross-correlations between ions indicated that the motions of $Me^+$ and TFSI ions are positively correlated; therefore they contribute destructively to the conductivity. As a consequence, the transference numbers of $Me^+$ ions are negative. This effect was observed in all simulations in both FFs, regardless of the Me cation, structure, and dynamics of its solvation shell.

Our results reinforce the recent computational findings[26,27] that the effect of negative effective transference numbers of $Li^+$ ions in ILs observed experimentally[17] is a general feature of metal salt solutions in ILs caused by strong correlations between motions of $Me^+$ and IL anions. This phenomenon affects the ion transport in the electrolyte, and as such, it is important for the design and optimization of electrolytes for Me-ion cells. Therefore, further experimental studies and more computational simulations are necessary to gain a better understanding and possibly more control over the effect.

## ■ ASSOCIATED CONTENT

### Supporting Information

The Supporting Information is available free of charge at https://pubs.acs.org/doi/10.1021/acs.jpcb.9b10391.

Compositions of investigated systems, abundance of different combinations of $N_O$ and $N_{an}$ values, residence time autocorrelation functions for TFSI anions, sample fits of the time autocorrelation functions, sample plot of collective MSD, contributions to the $\sigma_{c-c}$ component of the conductivity, effective charges of metal cations, and parameters of the FFs (PDF)

## ■ AUTHOR INFORMATION


### Corresponding Author

*E-mail: eilmes@chemia.uj.edu.pl.

### ORCID

Piotr Kubisiak: 0000-0002-2680-2461

Piotr Wróbel: 0000-0003-0852-8427

Andrzej Eilmes: 0000-0002-4690-2611


### Notes

The authors declare no competing financial interest.

## ■ ACKNOWLEDGMENTS

This work was supported by the National Science Centre (Poland) grant no. UMO-2016/21/B/ST4/02110. The PL-Grid infrastructure was used in computations.

## ■ REFERENCES


(1) Li, M.; Lu, J.; Chen, Z.; Amine, K. 30 Years of Lithium-Ion Batteries. *Adv. Mater.* **2018**, *30*, 1800561.

(2) Zubi, G.; Dufo-López, R.; Carvalho, M.; Pasaoglu, G. The Lithium-Ion Battery: State of the Art and Future Perspectives. *Renewable Sustainable Energy Rev.* **2018**, *89*, 292−308.

(3) Kim, T.; Song, W.; Son, D.-Y.; Ono, L. K.; Qi, Y. Lithium-Ion Batteries: Outlook on Present, Future, and Hybridized Technologies. *J. Mater. Chem. A* **2019**, *7*, 2942−2964.

(4) Etacheri, V.; Marom, R.; Elazari, R.; Salitra, G.; Aurbach, D. Challenges in the Development of Advanced Li-Ion Batteries: A Review. *Energy Environ. Sci.* **2011**, *4*, 3243−3262.

(5) Xu, K. Electrolytes and Interphases in Li-Ion Batteries and Beyond. *Chem. Rev.* **2014**, *114*, 11503−11618.

(6) Xue, Z.; He, D.; Xie, X. Poly(ethylene oxide)-Based Electrolytes for Lithium-Ion Batteries. *J. Mater. Chem. A* **2015**, *3*, 19218−19253.

(7) Marcinek, M.; Syzdek, J.; Marczewski, M.; Piszcz, M.; Niedzicki, L.; Kalita, M.; Plewa-Marczewska, A.; Bitner, A.; Wieczorek, P.; Trzeciak, T.; et al. Electrolytes for Li-Ion Transport − Review. *Solid State Ionics* **2015**, *276*, 107−126.

(8) Palomares, V.; Serras, P.; Villaluenga, I.; Hueso, K. B.; Carretero-González, J.; Rojo, T. Na-Ion Batteries, Recent Advances and Present Challenges to Become Low Cost Energy Storage Systems. *Energy Environ. Sci.* **2012**, *5*, 5884−5901.

(9) Yabuuchi, N.; Kubota, K.; Dahbi, M.; Komaba, S. Research Development on Sodium-Ion Batteries. *Chem. Rev.* **2014**, *114*, 11636−11682.

(10) Slater, M. D.; Kim, D.; Lee, E.; Johnson, C. S. Sodium-Ion Batteries. *Adv. Funct. Mater.* **2013**, *23*, 947−958.




DOI: 10.1021/acs.jpcb.9b10391
J. Phys. Chem. B 2020, 124, 413−421

(11) Peters, J.; Buchholz, D.; Passerini, S.; Weil, M. Life Cycle Assessment of Sodium-Ion Batteries. *Energy Environ. Sci.* **2016**, *9*, 1744−1751.
(12) Ponrouch, A.; Monti, D.; Boschin, A.; Steen, B.; Johansson, P.; Palacín, M. R. Non-Aqueous Electrolytes for Sodium-Ion Batteries. *J. Mater. Chem. A* **2015**, *3*, 22−42.
(13) Watanabe, M.; Thomas, M. L.; Zhang, S.; Ueno, K.; Yasuda, T.; Dokko, K. Application of Ionic Liquids to Energy Storage and Conversion Materials and Devices. *Chem. Rev.* **2017**, *117*, 7190−7239.
(14) Yang, Q.; Zhang, Z.; Sun, X.-G.; Hu, Y.-S.; Xing, H.; Dai, S. Ionic Liquids and Derived Materials for Lithium and Sodium Batteries. *Chem. Soc. Rev.* **2018**, *47*, 2020−2064.
(15) Forsyth, M.; Porcarelli, L.; Wang, X.; Goujon, N.; Mecerreyes, D. Innovative Electrolytes Based on Ionic Liquids and Polymers for Next-Generation Solid-State Batteries. *Acc. Chem. Res.* **2019**, *52*, 686−694.
(16) Ponrouch, A.; Marchante, E.; Courty, M.; Tarascon, J.-M.; Palacín, M. R. Search of an Optimized Electrolyte for Na-Ion Batteries. *Energy Environ. Sci.* **2012**, *5*, 8572−8583.
(17) Gouverneur, M.; Schmidt, F.; Schönhoff, M. Negative Effective Li Transference Numbers in Li Salt/Ionic Liquid Mixtures: Does Li Drift in the "Wrong" Direction? *Phys. Chem. Chem. Phys.* **2018**, *20*, 7470−7478.
(18) Lesch, V.; Li, Z.; Bedrov, D.; Borodin, O.; Heuer, A. The Influence of Cations on Lithium Ion Coordination and Transport in Ionic Liquid Electrolytes: a MD Simulation Study. *Phys. Chem. Chem. Phys.* **2016**, *18*, 382−392.
(19) Borodin, O.; Giffin, G. A.; Moretti, A.; Haskins, J. B.; Lawson, J. W.; Henderson, W. A.; Passerini, S. Insights into the Structure and Transport of the Lithium, Sodium, Magnesium, and Zinc Bis-(trifluoromethansulfonyl)imide Salts in Ionic Liquids. *J. Phys. Chem. C* **2018**, *122*, 20108−20121.
(20) Ray, P.; Balducci, A.; Kirchner, B. Molecular Dynamics Simulations of Lithium-Doped Ionic-Liquid Electrolytes. *J. Phys. Chem. B* **2018**, *122*, 10535−10547.
(21) Chen, F.; Howlett, P.; Forsyth, M. Na-Ion Solvation and High Transference Number in Superconcentrated Ionic Liquid Electrolytes: A Theoretical Approach. *J. Phys. Chem. C* **2018**, *122*, 105−114.
(22) Wróbel, P.; Kubisiak, P.; Eilmes, A. Interactions in Sodium Bis(fluorosulfonyl)imide/1-Ethyl-3-methylimidazolium Bis-(fluorosulfonyl)imide Electrolytes for Na-Ion Batteries: Insights from Molecular Dynamics Simulations. *J. Phys. Chem. C* **2019**, *123*, 14885−14894.
(23) Huang, Q.; Lourenço, T. C.; Costa, L. T.; Zhang, Y.; Maginn, E. J.; Gurkan, B. Solvation Structure and Dynamics of $Li^+$ in Ternary Ionic Liquid−Lithium Salt Electrolytes. *J. Phys. Chem. B* **2019**, *123*, 516−527.
(24) Oldiges, K.; Diddens, D.; Ebrahiminia, M.; Hooper, J. B.; Cekic-Laskovic, I.; Heuer, A.; Bedrov, D.; Winter, M.; Brunklaus, G. Understanding Transport Mechanisms in Ionic Liquid/Carbonate Solvent Electrolyte Blends. *Phys. Chem. Chem. Phys.* **2018**, *20*, 16579−16591.
(25) Dong, D.; Sälzer, F.; Roling, B.; Bedrov, D. How Efficient is $Li^+$ Ion Transport in Solvate Ionic Liquids under Anion-blocking Conditions in a Battery? *Phys. Chem. Chem. Phys.* **2018**, *20*, 29174−29183.
(26) Molinari, N.; Mailoa, J. P.; Craig, N.; Christensen, J.; Kozinsky, B. Transport Anomalies Emerging from Strong Correlation in Ionic Liquid Electrolytes. *J. Power Sources* **2019**, *428*, 27−36.
(27) Molinari, N.; Mailoa, J. P.; Kozinsky, B. General Trend of a Negative Li Effective Charge in Ionic Liquid Electrolytes. *J. Phys. Chem. Lett.* **2019**, *10*, 2313−2319.
(28) Kubisiak, P.; Eilmes, A. Molecular Dynamics Simulations of Ionic Liquid Based Electrolytes for Na-Ion Batteries: Effects of Force Field. *J. Phys. Chem. B* **2017**, *121*, 9957−9968.
(29) Martínez, L.; Andrade, R.; Birgin, E. G.; Martínez, J. M. Packmol: A Package for Building Initial Configurations for Molecular Dynamics Simulations. *J. Comput. Chem.* **2009**, *30*, 2157−2164.
(30) Phillips, J. C.; Braun, R.; Wang, W.; Gumbart, J.; Tajkhorshid, E.; Villa, E.; Chipot, C.; Skeel, R. D.; Kalé, L.; Schulten, K. Scalable Molecular Dynamics with NAMD. *J. Comput. Chem.* **2005**, *26*, 1781−1802.
(31) Brela, M. Z.; Kubisiak, P.; Eilmes, A. Understanding the Structure of the Hydrogen Bond Network and Its Influence on Vibrational Spectra in a Prototypical Aprotic Ionic Liquid. *J. Phys. Chem. B* **2018**, *122*, 9527−9537.
(32) Jorgensen, W. L.; Maxwell, D. S.; Tirado-Rives, J. Development and Testing of the OPLS All-Atom Force Field on Conformational Energetics and Properties of Organic Liquids. *J. Am. Chem. Soc.* **1996**, *118*, 11225−11236.
(33) Canongia Lopes, J. N.; Deschamps, J.; Pádua, A. A. H. Modeling Ionic Liquids Using a Systematic All-Atom Force Field. *J. Phys. Chem. B* **2004**, *108*, 2038−2047.
(34) Köddermann, T.; Paschek, D.; Ludwig, R. Molecular Dynamic Simulations of Ionic Liquids: A Reliable Description of Structure, Thermodynamics and Dynamics. *ChemPhysChem* **2007**, *8*, 2464−2470.
(35) Jensen, K. P.; Jorgensen, W. L. Halide, Ammonium, and Alkali Metal Ion Parameters for Modeling Aqueous Solutions. *J. Chem. Theory Comput.* **2006**, *2*, 1499−1509.
(36) Lamoreux, G.; Roux, B. Modeling Induced Polarization with Classical Drude Oscillators: Theory and Molecular Dynamics Simulation Algorithm. *J. Chem. Phys.* **2003**, *119*, 3025−3039.
(37) Borodin, O. Polarizable Force Field Development and Molecular Dynamics Simulations of Ionic Liquids. *J. Phys. Chem. B* **2009**, *113*, 11463−11478.
(38) Feller, S. E.; Zhang, Y.; Pastor, R. W.; Brooks, B. R. Constant Pressure Molecular Dynamics Simulation: The Langevin Piston Method. *J. Chem. Phys.* **1995**, *103*, 4613−4621.
(39) Martyna, G. J.; Tobias, D. J.; Klein, M. L. Constant Pressure Molecular Dynamics Algorithms. *J. Chem. Phys.* **1994**, *101*, 4177−4189.
(40) Darden, T.; York, D.; Pedersen, L. Particle Mesh Ewald: An Nlog(N) Method for Ewald Sums in Large Systems. *J. Chem. Phys.* **1993**, *98*, 10089−10092.
(41) Monti, D.; Jónsson, E.; Palacín, M. R.; Johansson, P. Ionic Liquid Based Electrolytes for Sodium-Ion Batteries: $Na^+$ Solvation and Ionic Conductivity. *J. Power Sources* **2014**, *245*, 630−636.
(42) Seki, S.; Kobayashi, Y.; Miyashiro, H.; Ohno, Y.; Usami, A.; Mita, Y.; Kihira, N.; Watanabe, M.; Terada, N. Lithium Secondary Batteries Using Modified-Imidazolium Room-Temperature Ionic Liquid. *J. Phys. Chem. B* **2006**, *110*, 10228−10230.
(43) Kashyap, H. K.; Annapureddy, H. V. R.; Raineri, F. O.; Margulis, C. J. How Is Charge Transport Different in Ionic Liquids and Electrolyte Solutions? *J. Phys. Chem. B* **2011**, *115*, 13212−13221.
(44) Yeh, I.-C.; Hummer, G. System-Size Dependence of Diffusion Coefficients and Viscosities from Molecular Dynamics Simulations with Periodic Boundary Conditions. *J. Phys. Chem. B* **2004**, *108*, 15873−15879.
(45) Gabl, S.; Schröder, C.; Steinhauser, O. Computational Studies of Ionic Liquids: Size Does Matter and Time Too. *J. Chem. Phys.* **2012**, *137*, 094501.


DOI: 10.1021/acs.jpcb.9b10391
*J. Phys. Chem. B* 2020, 124, 413−421